Available online at www.eccomasproceedia.org
Eccomas Proceedia COMPDYN (2021) 3942-3956

ECCOMAS
Proceedia

COMPDYN 2021
8th ECCOMAS Thematic Conference on
Computational Methods in Structural Dynamics and Earthquake Engineering
M. Papadrakakis, M. Fragiadakis (eds.)
Streamed from Athens, Greece, 28 - 30 June 2021

# AN ADVANCED MODEL FOR THE FLUID VISCOUS DAMPER BRITTLE FAILURE

**L. Gioiella[1], F. Scozzese[1], E. Tubaldi[2], L. Ragni[3], and A. Dall'Asta[1]**

[1] SAAD, University of Camerino
Viale della Rimembranza 3, 63100 Ascoli Piceno (AP), Italy
{laura.gioiella, fabrizio.scozzese, andrea.dallasta}@unicam.it

[2] Department of Civil and Environmental Engineering, University of Strathclyde
75 Montrose Street, Glasgow G1 1XJ, Scotland, UK
enrico.tubaldi@strath.ac.uk

Department of Civil and Building Engineering and Architecture, Università Politecnica delle Marche
Via Brecce Bianche Ancona, Italy
laura.ragni@univpm.it

## Abstract

*Fluid viscous dampers have proven to be a very efficient solution for reducing the seismic demand on structural and non-structural components, for both new and existing structures. Nowadays, the topics, which need to be further investigated, deal with the reliability and robustness of such kind of energy dissipating devices. Damper failures are generally brittle mechanisms, which can compromise the capacity of the structure to withstand the seismic action, leading to a lack of robustness of the overall system.*

*In this study, an advanced model, which is able to describe the fluid viscous damper brittle failure, has been developed in OpenSees and is discussed. The failure of a damper is related to the exceedance of its strength capacity and can be attained because of the forces arising related to the end-stroke impact or can be due to excessive piston velocity (over-velocity). The effect of damper failure on the seismic performance of the structural system is investigated by performing multi-stripe analyses and monitoring different global and local demand parameters. The proposed model for the damper is applied to a benchmark structure, consisting on a 3-storey steel moment resisting frame.*

**Keywords:** Viscous Dampers; End-stroke; Over-velocity; Brittle Failure; Seismic Risk; Reliability.

ISSN:2623-3347 
Peer-review under responsibility of the organizing committee of COMPDYN 2021.
doi: 10.7712/120121.8758.18946

## 1 INTRODUCTION

Fluid viscous dampers (FVDs) are devices widely used for seismic passive protection of both new and existing structures. They are widely employed for reducing displacements and interstorey drift demands in newly-designed structures as well as in existing ones by using both external and internal configurations [1]-[8].

Several approaches are to date available for designing both size and location of viscous dampers within a building frame based on direct procedures [1][9][10][11][12] or optimization methods [13][14]. These design approaches generally allow to control the seismic performance of buildings under the design seismic intensity level. However, the reliability under extreme, low-probability earthquake events may be characterized by low robustness and inadequate safety levels because dampers usually exhibit a brittle collapse behaviour and their failure may trigger the collapse of the whole system. As a consequence, more accurate studies simulating the effect of the device failure should be carried out to provide a better evaluation of the structural reliability under strong earthquakes.

In order to shed light on this aspect, the present paper introduces a model able at describing the brittle failure of FVD devices and its influence on the structural reliability. The collapse is due to the attainment of the force capacity of the damper, related to the over-velocity or to the achievement of the end-stroke. In particular, it is assumed that a brittle failure occurs in the device once the maximum force is attained, consistently with the viscous damper numerical model proposed in [15]. This way, the proposed model can be suitable to describe the consequences of the failure of the devices on the seismic performance of structural systems and also to evaluating the probability of collapse of structures equipped with dampers, through risk analyses performed by using probabilistic approaches [16]-[24].

Recent probabilistic analyses, indeed, have already investigated some specific issues, such as the effect of ground motion variability on the response of systems equipped with either linear and nonlinear viscous dampers [19][20][21]; the influence of the degree of nonlinearity of the dampers [20][22], and the effect of the damper parameters variability [22][23][24] stemming from the device manufacturing process, as acknowledged by the main international Standards for seismic structural design [25][26][27][28]. However, in these studies the device failure was not explicitly taken into account.

The proposed model is firstly described in the following section and then it is applied to a three-storey steel building case study, already considered as benchmark structure in previous studies (SAC Phase II Steel Project, [29]). For consistency with the adopted benchmark case study, the seismic hazard is also assumed equal to the one of [29]. The dissipative system is dimensioned to provide an added damping equal to 30%, using both linear and nonlinear devices, by varying their degree of nonlinearity among two boundary values. The capacity of the dampers (stroke and strength) is evaluated at the design condition, corresponding to a seismic action with Mean Annual Frequency (MAF) of exceeding equal to $2 \cdot 10^{-3}$.

Some preliminary results under increasing harmonic load histories are reported to illustrate the model capabilities and the sequence of failures triggered by the damper failure. Subsequently, few selected results from Multi Stripe Analysis (MSA) are also presented to illustrate overall the problem of damper failure and related effects on the structural performance of the case study. Finally, a preliminary evaluation of the overall probabilistic response is provided. Results obtained by considering the failure of the dampers are compared with those achieved with two limit cases, that is the condition of no failure, where no damper's failure is permitted and the bare frame, which represents the building without FVDs.

Further details regarding fragility curves and demand hazard curves, where the structural performance is analysed considering MAF of exceeding up to $10^{-5}$ 1/yr, can be found in [30].

## 2 FLUID VISCOUS DAMPERS MODELLING

The constitutive law of a fluid viscous damper (FVD) can be described through the following relationship [15][31]:

$$F_d(v) = c|v|^{\alpha} sgn(v) \tag{1}$$

where $v$ is the relative velocity between the device ends, $F_d$ is the damper resisting force, $|v|$ is the absolute value of $v$, $sgn$ is the sign operator, $c$ and $\alpha$ are two constitutive parameters: the former is an amplification factor, while the latter describes the damper nonlinear behaviour.

It is worth noting that viscous dampers can be produced with $\alpha$ values ranging from 0.1 and 2. Devices with $\alpha > 1$ are not dissipative and are used as shock transmitters. Devices with $0.1 \leq \alpha \leq 1.0$ are all potentially suitable for seismic energy dissipation, among these values, the range $0.3 \leq \alpha \leq 1.0$ is the most widespread [32][33][34][35].

A fluid viscous damper generally consists of a steel cylinder filled of a silicone fluid, within which a steel piston with small orifices on its head can move. In case of seismic events, the fluid is forced to pass through the orifices, moving from one side to the opposite side of the cylinder, thus dissipating into heat the input mechanical energy. The higher is the velocity of the movement, the greater is the dissipated energy. The cylinder is equipped with spherical hinges at its ends to avoid device bending. FVDs are generally connected to the structure by a stiff connection, consisting in a driver brace, dimensioned using an over-strength factor with respect to the viscous device. The stiffness of the driver brace is an important feature, because it needs to be sufficiently high to allow the device to be effective in dissipating energy. Further details on the damper components and their behaviour can be found in [15].

The failure of a damper is related to the exceedance of its strength capacity and can be attained because of the forces related to the end-stroke impact or can be due to excessive piston velocity. According to the described behaviour, dampers are generally classified and tested with reference to two characteristic parameters: the maximum values of stroke $\Delta_{d,max}$, and the maximum transmissible force $F_{d,max}$.

The end-stroke can be attained both in tension (maximum elongation of the device) and in compression (maximum shortening of the device). During a seismic event with an intensity higher than the design level of the device, it may happen that the device exploits the entire available stroke, resulting in an impact. At the instant of the impact, the velocity becomes null and the force notably increases, however, the attainment of the impact does not strictly imply the damper failure because the impact force may be lower than the device strength.

The second mechanism refers to the attainment of the maximum viscous force due to an excessive value of the velocity of the piston (over-velocity with respect to the design value). This extreme value of the force can induce a leak of the fluid or can damage the damper components, resulting in the failure of the device. It is noteworthy that once the maximum capacity $\left(F_{d,max}\right)$ is attained, the resulting failure mechanisms is brittle, thus making the device ineffective, with no residual ability to sustain loads or dissipate energy.

The model, proposed hereinafter, aims to describe the two aforesaid mechanisms using the damper model, depicted in Figure 1. It is composed of three elements: a dashpot, describing the dissipative behaviour; a hook and gap element, set in parallel to the dissipative device, which simulate the impact due to either excessive shortening ($-\Delta_{d,max}$) or elongation ($+\Delta_{d,max}$); and a third element, set in series with the others, simulating the failure due to the attainment of the force capacity. In this paper, the strength capacity is assumed to be the same in traction and in compression and the failure occurs when the modulus of damper force attains the limit value $F_{d,max}$.

The damper model discussed above is implemented in OpenSees [36] using two-node link elements simulating each of the three components, while various material properties are used to describe the different behaviours. A "Viscous material" is used for the dissipative element, by assigning the values of the constitutive parameters $c$ and $\alpha$. An "ElasticMultilinear material" depicts the force-displacement relationship related to impacts occurring both for elongation and shortening. Finally, a "MinMax material" is used to simulate the brittle failure, assigning the value of the strength capacity $F_{d,max}$. The stiffness of the "MinMax material" can be used to model the overall deformability of damper, connections, and brace. However, once the strength capacity is reached, the element fails and does not provide any more contribution in terms of reaction force.

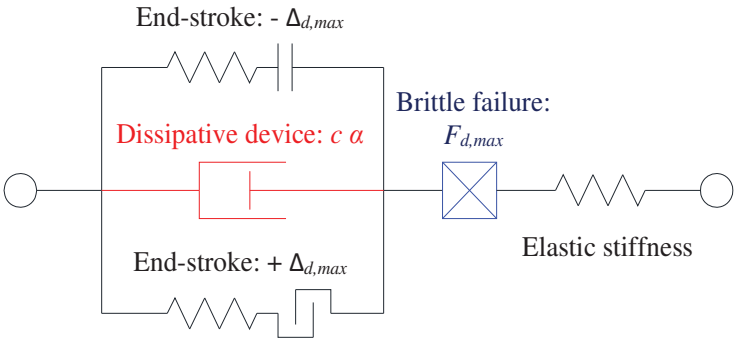


Figure 1: Dissipative device model encompassing the failure mechanisms.

## 3 CASE STUDY

In this section, the case study, dealing with a steel moment-resisting frame structure representative of low-rise buildings is introduced together with the considered seismic scenario. The frame is equipped with FVDs with both linear and non-linear behaviour that is values of the damper exponent $\alpha$ corresponding to 1.0 and 0.3.

### 3.1 Benchmark structure and hazard scenario

The three-storey building selected as case study is a steel moment resisting frame designed within the SAC-FEMA project with reference to gravity, wind and seismic load in compliance to the code requirement. It has been also widely used as benchmark structure in several studies concerning structural response control (e.g., [2][29][20]). The structural system of the building consists of perimeter moment-resisting frames and internal gravity frames with shear connections. The finite element model of the building (Figure 2) is a two-dimensional model representative of the weak and short direction of the building and has been developed in OpenSees following a non-linear fiber distributed approach, whose details can be found in [30].

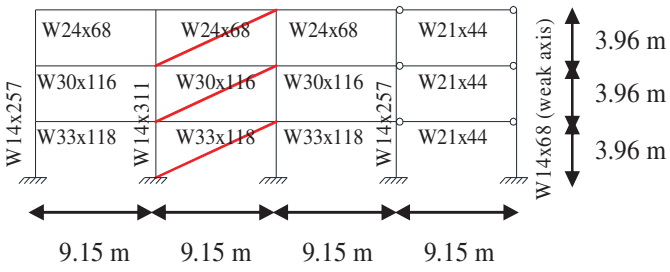


Figure 2: Building model descriptions: locations of the dampers (in red) and cross-sections of the members.

For consistency with the adopted benchmark case study, the hazard model and the related IM hazard curves are taken from [29]; however, the curves have been slightly extrapolated to make sure that the system failure probabilities can be accurately estimated, by following the recommendation of [37] about the optimal *IM* curve truncation for an accurate risk estimation via MSA analysis. The spectral pseudo-acceleration $S_a(T_1)$ of a linear elastic SDOF system with 2% damping ratio and fundamental vibration period equal to that of the structure $T_1$ is considered as intensity measure (*IM*). MSA is performed at 20 *IM* levels, with a set of 30 ground motions per each intensity level taken from the 60 records used in the SAC project [2].

For what concerns the FVDs design, this is carried out by considering the set of 30 records corresponding to a MAF of exceedance $\nu_{design} = \nu_{IM}(im_{design}) = 0.0021$ 1/yr. Further details and features of these records can be found in [30].

### 3.2 Damping system

The design of the FVDs is carried out to enhance the performance of the building under a seismic scenario with a 10% probability of exceedance in 50 years (ULS scenario according to Eurocode 8). To this aim, a target value $\xi_{add} = 30\%$ has been chosen for supplemental damping. In the present study, the damping coefficients of the linear devices have been distributed proportionally to the storey shear of the first mode of the bare frame.

Once determined the damping coefficients of the devices for the linear case, the viscous coefficients for the nonlinear FVDs corresponding to given value of the exponent $\alpha$, are evaluated following the approach outlined in [9][38][39] and based on the equivalence of the energies dissipated by the linear and nonlinear FVDs. It is noteworthy that the maximum interstorey drift along the building height without dampers, averaged over the 30 records considered, is equal to 3%, while with the addition of the dampers, it becomes 1.2%.

Table 1 and Table 2 report, respectively, the damping properties and the design parameters of the FVDs of the three elevations of the building for both the values of the constitutive parameter $\alpha$. Further details concerning the dissipative devices design can be found in [30].

| $\alpha$ | $c_1$ | $c_2$ | $c_3$ |
|---|---|---|---|
| | $[kNs^\alpha/m^\alpha]$ | | |
| 1 | 13,780 | 11,914 | 7428 |
| 0.3 | 4669 | 4037 | 2517 |

Table 1: Damping properties for different levels of damper nonlinearity.

| $\alpha$ | $\Delta_{d,1}$ $[mm]$ | $\Delta_{d,2}$ $[mm]$ | $\Delta_{d,3}$ $[mm]$ | $F_{d,1}$ $[kN]$ | $F_{d,2}$ $[kN]$ | $F_{d,3}$ $[kN]$ |
|---|---|---|---|---|---|---|
| 1.0 | 35.4 | 44.5 | 37.1 | 3109 | 3336 | 1956 |
| 0.3 | 29.6 | 39.7 | 35.7 | 3044 | 2796 | 1712 |

Table 2: FVD design parameter at the design condition.

### 3.3 Amplification factors for the FVD control parameters

Modern seismic codes prescribe that anti-seismic devices shall be dimensioned starting from the values of the control parameters evaluated for seismic design actions having an assigned probability of exceedance. Then, the capacities of the devices are assigned amplifying these

control parameters, which are stroke and force for the FVDs, by means of amplification factors, or reliability factors, in order to ensure a target level of safety.

The amplification factors proposed by Codes are two and aim to control the two failure mechanisms discussed above. The former, here denoted by $\gamma_\Delta$, amplifies the maximum stroke measured at design condition. The amplified stroke must not exceed the damper capacity $\Delta_{d,max}$. The latter, here denoted by $\gamma_v$, amplifies the maximum velocity measured at design condition. Damper force is obtained by Eqn. (1) and must not exceed the damper capacity $F_{d,max}$.

Per each value of the constitutive parameter $\alpha$, five combinations of amplification factors relevant to damper stroke and strength are considered, ranging from 1.0 up to 3.0, considering also, the prescriptions of European codes [26][27] and American Standards [28]. Moreover, for comparison purposes, two more limit cases are considered: "No Failure" that is the case where no dampers' failures are permitted, and "Bare Model", which represents the frame without FVDs. Further details concerning the combinations of amplification factors can be found in [30].

## 4 SYSTEM RESPONSE UNDER AN INCREASING SINUSOIDAL INPUT

In this section, the results obtained for a sinusoidal ground motion of increasing intensity are presented. The FVDs response parameters at the design condition refer to linear devices ($\alpha = 1$) without amplification factors, that is $\gamma_v = \gamma_\Delta = 1.0$.

The choice of an increasing harmonic input motion is motivated by the fact that it allows to easily identify the attainment of the damper strength capacity through one of the two mechanisms, impact and over-velocity and the related consequences on the frame undergoing a more general time-history input motion.

Figure 3 shows the sinusoidal input having a period of 0.9 seconds and an initial magnitude of $1\ m/s^2$. The amplitude of the motion is constant for five cycles, after that it is increased with a coefficient equal to 1.5 and remains again constant for five cycles. The magnification of the motion amplitude is repeated four times, resulting in a motion that has five different amplitudes, with a maximum equal to $5\ m/s^2$, and that lasts 22.5 seconds. At the end of the input, there are few seconds, which are useful to understand how the case study restores its rest condition.

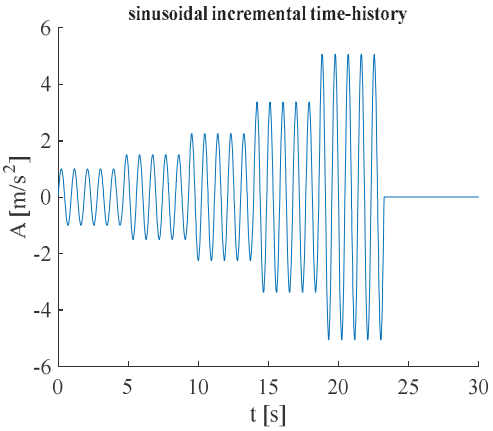


Figure 3: Sinusoidal incremental dynamic input.

Figure 4 a) and b) illustrate the time-history of the damper forces $F_{d,i}$ recorded along the height of the building. The black solid line refers to the device installed between the ground and the first floor, the red one refers to the intermediate device at the second storey, while the blue one represents the damper at the top storey. At the beginning of the third increment of the

sinusoidal input (between 14.4 and 14.5 seconds), graphs show some small ripples, which are more evident for the intermediate and top-storey devices (Figure 4 b), and they are caused by small impacts due to the end-stroke attainment. In this case, the impact occurs but it does not lead to the attainment of the damper strength capacity. At the time instant 14.6 s the damper placed at the first level reaches its force capacity due to over-velocity and its force drops to zero. Few instants later, also the other devices fail for over-velocity.

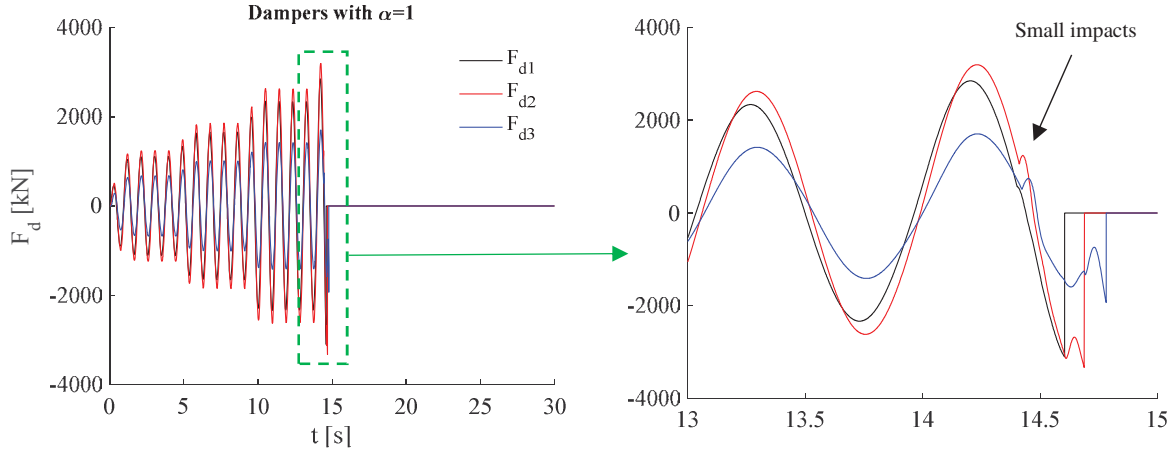


Figure 4: Time-history of the damper forces along the height of the building.

The effects of the damper failure can be deeper investigated through Figure 5 a) - c), where the stroke-force relationship ($\Delta_{d,i}$-$F_{d,i}$) of each device is shown. In particular, by observing these stroke-force relationships it is evident that at the beginning of the third increment of the input motion, all the three dampers experience the end-stroke attainment without failure, with impacts that are more evident for the intermediate and top-storey devices. After these impacts, occurred without consequences, the FVDs restore their behaviour as pure dissipative devices. Few instants later, suddenly, the damper located at the ground floor fails due to over-velocity (Figure 5 a), triggering the sequence of damper failures at the upper elevations. The sequence is highlighted by a series of ripples in the stroke-force relationship of the intermediate (Figure 5 b) and especially top-storey device (Figure 5 c). The ripples begin when the first device fails and last until all the devices fail for over-velocity.

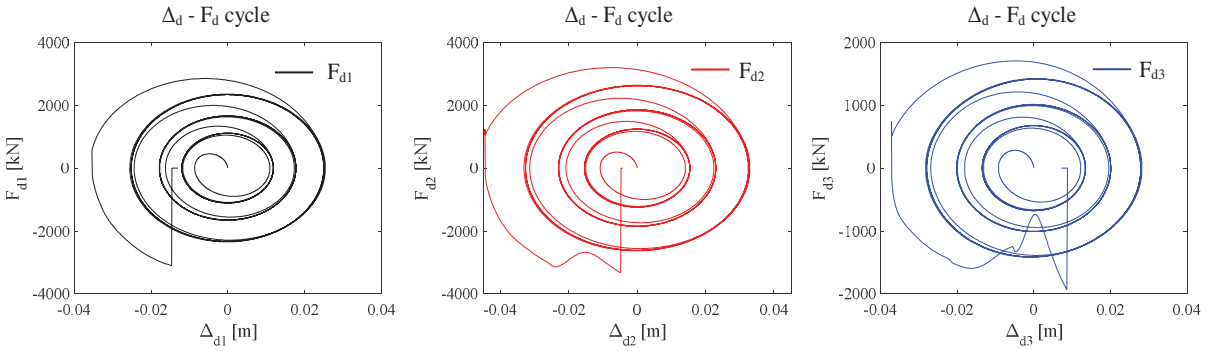


Figure 5: Stroke-force relationships of the devices.

Figure 6 a) - c) shows the time-histories of the parameters strictly related to the frame response, that is floor displacements $u_i$, floor relative velocities $v_{r,i}$ and floor absolute accelerations $A_i$, highlighting the consequences of the damper failures on the frame itself. Generally, all the responses are significantly amplified by the impacts occurring in the dampers and by their failure. The absolute accelerations (Figure 6 c) are more affected than the displacements (Figure 6 a). It is worth to note that the peaks in terms of absolute accelerations, recorded between 14 and 15 seconds, are mainly related to the impacts experimented by the devices before their failure.

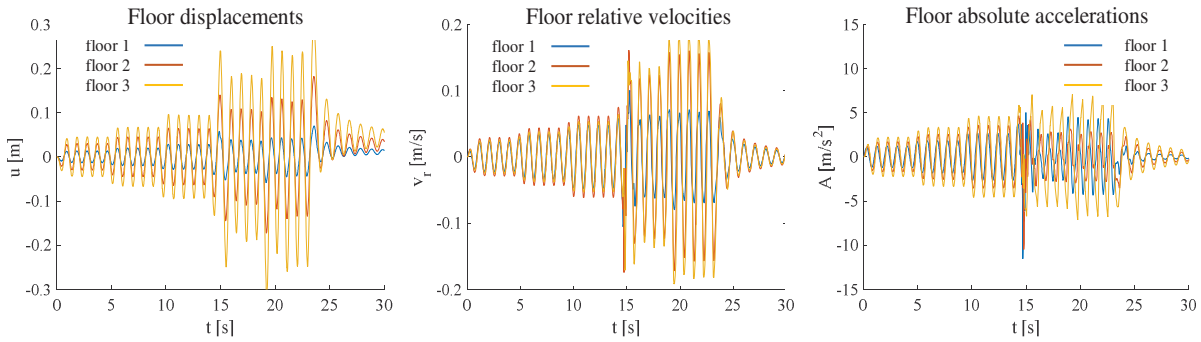


(a) (b) (c)

Figure 6: Time-histories of the response parameters of the frame.

## 5 SYSTEM SEISMIC RESPONSE

To shed further light on the consequences of FVDs failure, this subsection shows few selected information from MSA analyses to illustrate overall the problem of damper failure and related effects on the structural performance of the case study. The results refer to both low (*IM* level 5) and high (*IM* level 15) seismic intensities and for a single time-history (TH) analysis (TH 25).

Figure 7 a) and b) compares the time-histories of the interstorey-drift ratio (IDR) response of the bare model and of the system with linear and nonlinear dampers designed without amplification factors ($\gamma_v = \gamma_\Delta = \gamma = 1.0$) at both the seismic intensity levels. The response in terms of IDR at floor 1 is only discussed, given the high similarity of the response at all floors.

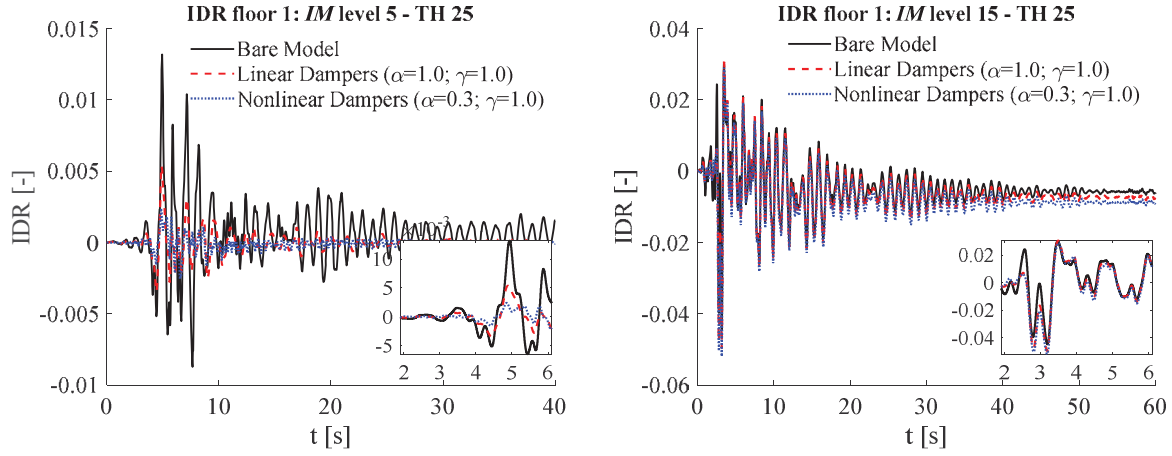


(a) (b)

Figure 7: Time histories of the IDR at *IM* level n. 5 (a) and (b) *IM* n. 15. Comparison between the bare model and the model with linear and nonlinear dampers (without amplification factors).

As already shown for the incremental harmonic input, it is confirmed that at lower seismic intensities FVDs are effective in damping the response, while the beneficial mitigation of the response provided by the dampers vanishes at higher *IM*s, due to their failure. At *IM* level 5, indeed, the response of the frame with FVDs is damped over the whole earthquake duration, since no device failure is observed at this intensity level. From the inset of Figure 7 (b), instead, it can be observed that dampers fail at around 2.5 seconds since the beginning of the time-history of *IM* level 15, therefore the IDR response is damped until that time instant, while later on the response tends towards the bare-frame response.

To deeply understand the FVDs behaviour along the height of the building, Figure 8 compares the time histories selected from the *IM* level 15 (higher intensity) of the force on dampers at all the three elevations of the building. Here dampers failure occurs quite simultaneously at 2.5 s, when the forces suddenly drop to zero and the dampers become ineffective.

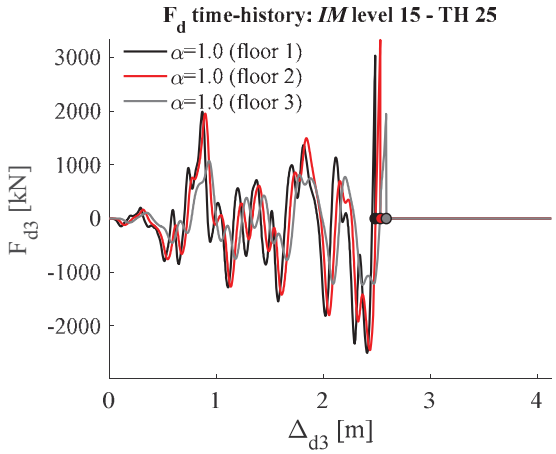


Figure 8: Failure time-lag among dampers at different floors.

For sake of completeness, the dampers force-stroke cyclic responses corresponding to the cases plotted in Figure 7 are shown in Figure 9 (*IM* level 5) and Figure 10 (*IM* level 15). In each figure a comparison is made between the responses of the linear (red dashed line) and nonlinear dampers (blue dotted line) at the first (figure a) and third storey (figure b). It is worth to observe that at *IM* level 5 (Figure 9 a) and b) there is no evidence of impact and the failure is never attained, thus complete cycles can be observed.

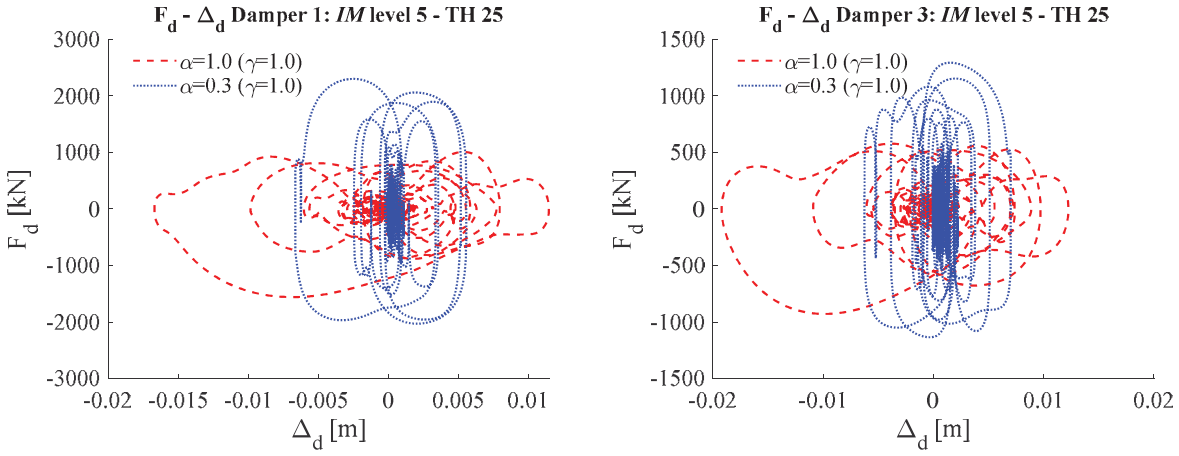


(a) (b)

Figure 9: Damper response at *IM* levels 15. Comparison between linear and nonlinear dampers (without amplification factors) at (a) first and (b) third floor

In Figure 10 a) and b), instead, the attainment of the maximum force capacity (hence the failure), for both linear and nonlinear dampers, is due to over-velocity because the force suddenly becomes null and the hysteretic cycle is sudden interrupted, without any impact.

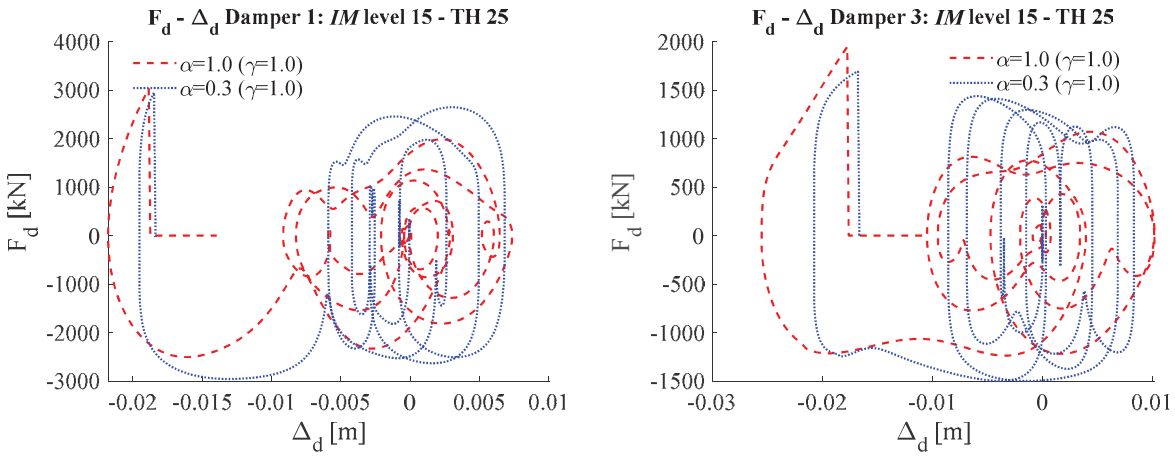


(a) (b)

Figure 10: Damper response at *IM* levels 15. Comparison between linear and nonlinear dampers (without amplification factors) at (a) first and (b) third floor.

## 5.1 Preliminary evaluation of the overall probabilistic response

This section provides a preliminary evaluation of the overall probabilistic response of the analysed case study in terms of global engineering demand parameters (EDPs). First, the median response of the building at different *IM* levels is presented, then the demand hazard curves, with respect to the mean annual rate of exceedance, $\nu_D$, of the same EDPs are introduced. The monitored parameters are the maximum interstorey drift (IDR) and the maximum absolute acceleration (A) recorded among the various storeys.

The median response of the building at different seismic intensities for the case of linear dampers ($\alpha = 1.0$) is compared in Figure 11. The comparison involves the following three cases: 1) bare model (black line); 2) building with dampers designed without amplification factors ($\gamma_v = \gamma_\Delta = 1$) (blue line); 3) building with no dampers' failure permitted ($\gamma_v = \gamma_\Delta = \infty$) (red line).

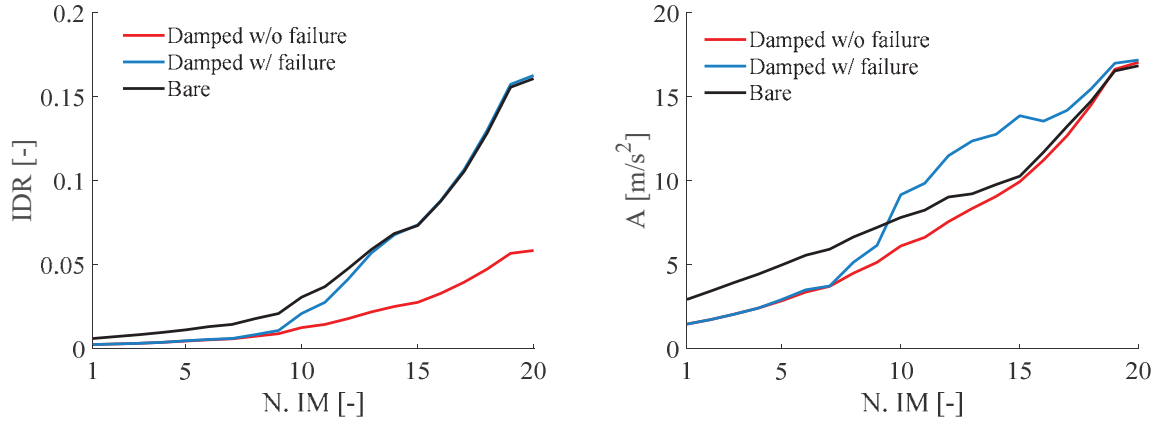


(a) (b)

Figure 11: Building response at different *IM* levels for the case with linear dampers ($\alpha$=1.0) in terms of (a) IDR and (b) A. Comparison between damped (with and without failure) and bare model.

Based on the results depicted in Figure 11 a) and b), it can be observed that the case of FVDs without failure notably reduces the response in terms of IDR up to the highest seismic intensities, while the beneficial effect in terms of acceleration mitigation is lower. On the other hand, in the case of FVDs that can fail, the IDR response of the damped systems tends to be almost that of the bare building once the devices are no longer effective (for *IM* levels higher than 10). The response in acceleration A, instead, shows peaks higher than the undamped frame system, due to the impacts induced by the devices end-stroke attainment.

Finally, Figure 12 a) and b) provides a first insight regarding the demand hazard curves of the maxima IDR and A among the storeys, with respect to the mean annual rate of exceedance $\nu_D$, for the linear dampers only ($\alpha = 1.0$).

The demand hazard curves compare the results achieved when accounting for different values of the amplification factors, previously introduced in section 3.3. The analysed cases are: dampers without amplification factors ($\gamma_v = \gamma_\Delta = 1.0$) (blue solid line) and dampers designed with different $\gamma$ factors, that is $\gamma_v = 1.5$ and $\gamma_\Delta = 1.0$ (brown solid line); $\gamma_v = \gamma_\Delta = 1.5$ (yellow solid line); $\gamma_v = \gamma_\Delta = 2.0$ (violet solid line); $\gamma_v = \gamma_\Delta = 3.0$ (green solid line). Moreover, the two limit cases of the bare frame model (black dashed line) and the damped model without damper failure (i.e., with $\gamma_\Delta = \gamma_v = \infty$) (red solid line) are also analysed for comparison purposes. Two horizontal dotted lines are also depicted in the charts, one identifying the design hazard level 0.0021 $yr^{-1}$ (black dotted line) and the other (red dotted line) denoting the target risk level desired for the structural systems ($2x10^{-4}$ $yr^{-1}$) [40][41].

With reference to Figure 12 a), it is worth to observe that when the dampers are designed with amplification factors larger than 1.0, the rate of exceeding of the target drift performance (IDR=0.012) is around 0.0021 $yr^{-1}$, the hazard level of the design action, with some slight deviations that can be justified by the probabilistic nature of the analysis. Once damper rupture is attained, the building response tends to that of the bare model (black dashed line) and the magnitude of the amplification factors governs the "rapidity" of the transition from the damped to the bare frame curve.

For what concerns the response in terms of absolute accelerations, instead, (Figure 12 b) they are lower than those of the bare frame until the dampers are effective, while they become even higher than that of the bare frame due to end-strokes impacts experienced by the dampers, before their failures for almost all the values of the amplification factors higher than 1.0. In this case also, the magnitude of the amplification factors determines the annual rate probability at which the response tends to become higher than that of the bare frame. Further details concerning the probabilistic analyses results can be found in [30].

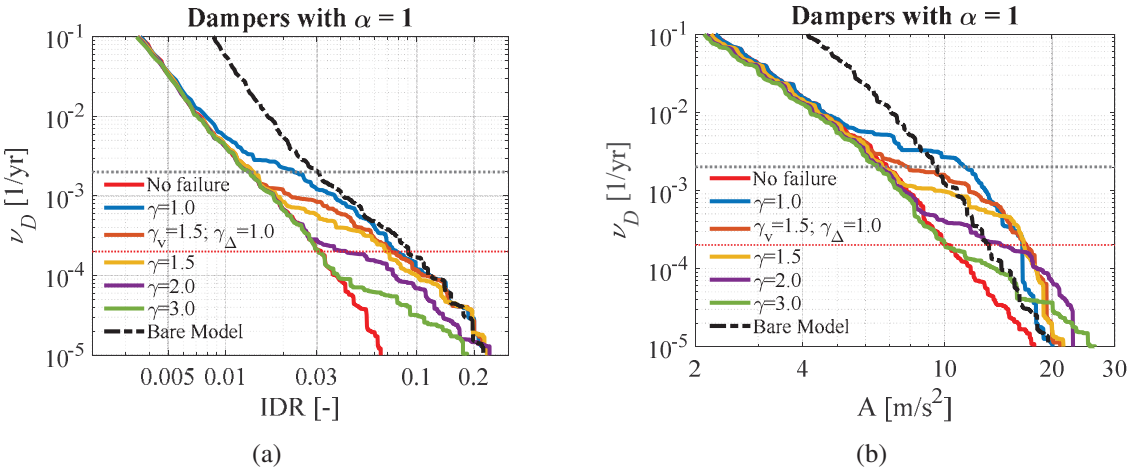


(a) (b)

Figure 12: Demand hazard curves of (a) IDR and (b) A for different damper amplification factors. Case of building with linear dampers ($\alpha = 1.0$).

## 6 CONCLUSIONS

The present paper introduces an advanced model which is able to describe the brittle failure of FVDs. Such kind of collapse occurs when the internal force of the device attains its strength capacity and this may occur for two reasons: impact when end-stroke is attained, or attainment of excessive velocity. Both these failure modalities are considered in the analyses.

As a general result, it is observed that combined effects of impacts and extreme velocities may induce a global brittle behaviour that cannot be perceived by models neglecting these phenomena. More specifically, the following conclusions can be drawn:

- The consequences of the damper failure on the performance of a structural system depend on the number of dampers remained active. If all dampers fail together, then the system response in terms of IDR tends to that of the bare building, while the one regarding absolute accelerations may be higher or even worse than that of the bare frame, as a consequence of impacts and dissipation concentrated at some storeys only.
- The magnitude of the amplification factors ($\gamma_{\Delta}, \gamma_{v}$) adopted for damper stroke and velocity, governs the "rapidity" of the response transition from damped, or partially damped.
- If no amplification is provided ($\gamma_{v} = \gamma_{\Delta} = 1.0$), the dampers probability of failure is higher than the design hazard level (assumed in this work equal to 0.0021 $yr^{-1}$), thus, dampers experience failure at intensity levels lower than the design one.
- The use of amplification factors higher than 1.0 allows attaining lower failure probabilities, and this beneficial effect is more significant for larger $\gamma$–factors.

## REFERENCES

[1] Tubaldi, E., Gioiella, L., Scozzese, F., Ragni, L., & Dall'Asta, A. (2020). A design method for viscous dampers connecting adjacent structures. *Frontiers in Built Environment*, *6*, 25.

[2] Barroso LR. Performance evaluation of vibration controlled steel structures under seismic loads. PhD thesis, Stanford University, California, US, 1999.

[3] Pavlou, E, Constantinou, M.C., 2006. Response of Nonstructural Components in Structures with Damping Systems, *Journal of Structural Engineering*, **132**(7), 1108-1117.

[4] Lavan, O, Dargush, G.F., 2009. Multi-Objective Evolutionary Seismic Design with Passive Energy Dissipation Systems, *Journal of Earthquake Engineering*, **13**(6), 758-790.

[5] Gioiella, L., Tubaldi, E., Gara, F., Dezi, L., Dall'Asta, A. (2018). Modal properties and seismic behaviour of buildings equipped with external dissipative pinned rocking braced frames. *Engineering Structures, 172*. https://doi.org/10.1016/j.engstruct.2018.06.043

[6] Pavia, A., Scozzese, F., Petrucci, E., & Zona, A. (2021). Seismic Upgrading of a Historical Masonry Bell Tower through an Internal Dissipative Steel Structure. Buildings, 11(1), 24.

[7] Gioiella, L., Tubaldi, E., Gara, F., Dezi, L., Dall'Asta, A. (2018). Stochastic Seismic Analysis and Comparison of Alternative External Dissipative Systems. *Shock and Vibrations, 47*. https://doi.org/10.1155/2018/5403737

[8] Tubaldi, E. (2015). Dynamic behavior of adjacent buildings connected by linear viscous/viscoelastic dampers. *Structural Control and Health Monitoring*, **22**(8), 1086-1102.

[9] Hwang, JS., Lin, WC., Wu, NJ. (2010). Comparison of distribution methods for viscous damping coefficients to building. *Structure and Infrastructure Engineering: Maintenance, Management, Life-Cycle Design and Performance, 9*(1), 28-41. http://dx.doi.org/10.1080/15732479.2010.513713

[10] Silvestri, S., Palermo, M., & Trombetti, T. (2018). A direct procedure for the seismic design of frame structures with added viscous dampers. *Seismic Resistant Structures*, 37.

[11] Tubaldi, E., Barbato, M., Dall'Asta, A., 2015. Efficient approach for the reliability-based design of linear damping devices for seismic protection of buildings. ASCE-ASME Journal of Risk and Uncertainty in Engineering Systems, Part A: Civil Engineering, 2(2), C4015009. DOI: 10.1061/AJRUA6.0000858.

[12] Palermo, M., Silvestri, S., Landi, L., Gasparini, G., & Trombetti, T. (2018). A "direct five-step procedure" for the preliminary seismic design of buildings with added viscous dampers. *Engineering Structures*, *173*, 933-950.

[13] Altieri, D., Tubaldi, E., De Angelis, M., Patelli, E., & Dall'Asta, A. (2018). Reliability-based optimal design of nonlinear viscous dampers for the seismic protection of structural systems. *Bulletin of Earthquake Engineering*, *16*(2), 963-982.

[14] Pollini, N., Lavan, O., & Amir, O. (2018). Optimization-based minimum-cost seismic retrofitting of hysteretic frames with nonlinear fluid viscous dampers. *Earthquake Engineering & Structural Dynamics*, *47*(15), 2985-3005.

[15] Miyamoto, H. K., Gilani, A. S., Wada, A., & Ariyaratana, C. (2010). Limit states and failure mechanisms of viscous dampers and the implications for large earthquakes. *Earthquake Engineering & Structural Dynamics, 39*, 1279-1297.

[16] Seo, C.Y., Karavasilis, T.L., Ricles, J.M, Sause, R., 2014. Seismic performance and probabilistic collapse resistance assessment of steel moment resisting frames with fluid viscous dampers, Earthquake Engineering and Structural Dynamics, 43(14), 2135-2154.

[17] Gidaris, I., Taflanidis, A.A., 2015. Performance assessment and optimization of fluid viscous dampers through life-cycle cost criteria and comparison to alternative design approaches. Bulletin of Earthquake Engineering, 13, 1003-1028.

[18] Tubaldi, E., Barbato, M., Dall'Asta, A., 2014. Performance-based seismic risk assessment for buildings equipped with linear and nonlinear viscous dampers. Engineering Structures, 78, 90-99.

[19] Tubaldi, E., Kougioumtzoglou, I.A., 2015. Nonstationary stochastic response of structural systems equipped with nonlinear viscous dampers under seismic excitation. Earthquake Engineering and Structural Dynamics, 44(1): 121–138.

[20] Dall'Asta, A., Tubaldi, E., Ragni, L., 2016. Influence of the nonlinear behaviour of viscous dampers on the seismic demand hazard of building frames. Earthquake Engineering and Structural Dynamics, 45(1), 149-169.

[21] Tubaldi, E., Ragni, L., Dall'Asta, A., 2015. Probabilistic seismic response assessment of linear systems equipped with nonlinear viscous dampers. Earthquake Engineering & Structural Dynamics, **44** (1), 101-120. DOI: 10.1002/eqe.2461

[22] Dall'Asta, A., Scozzese, F., Ragni, L., Tubaldi, E., 2017. Effect of the damper property variability on the seismic reliability of linear systems equipped with viscous dampers.

Bulletin of Earthquake Engineering, 15(11), 5025-5053. DOI 10.1007/s10518-017-0169-8

[23] Lavan, O., Avishur, M., 2013. Seismic behavior of viscously damped yielding frames under structural and damping uncertainties. Bulletin of Earthquake Engineering, 11(6), 2309–2332.

[24] Scozzese, F., Dall'Asta, A., Tubaldi, E., 2019. Seismic risk sensitivity of structures equipped with anti-seismic devices with uncertain properties, Structural Safety, 77, 30-47.

[25] American Society of Civil Engineers. Seismic Evaluation and Retrofit of Existing Buildings: ASCE Standard ASCE/SEI 41-17. American Society of Civil Engineers, 2017.

[26] European Committee for Standardization. EN 15129:2010 - Antiseismic devices, Brussels, Belgium, 2010

[27] European Committee for Standardization. Eurocode 8-Design of Structures for Earthquake Resistance. Part 1: General Rules, Seismic Actions and Rules for Buildings, Brussels, Belgium, 2004.

[28] ASCE (American Society of Civil Engineers). (2010). Minimum design loads for buildings and other structures. *Standard ASCE/SEI 7-10*.

[29] Barroso LR, Winterstein S. Probabilistic seismic demand analysis of controlled steel moment-resisting frame structures. *Earthquake Engineering and Structural Dynamics* 2002; 31(12):2049–2066.

[30] Scozzese, F., Gioiella, L., Tubaldi, E., Ragni, L., Dall'Asta, A., 2021. Influence of viscous dampers ultimate capacity on the seismic reliability of building structures. *Structural Safety* 2021. https://doi.org/10.1016/j.strusafe.2021.102096

[31] Constantinou, M. C., & Symans, M. D. (1992). Experimental and analytical investigation of seismic response of structures with supplemental fluid viscous dampers. Buffalo, NY: National Center for earthquake engineering research.

[32] Lee, D., & Taylor, D. P. (2001). Viscous damper development and future trends. The Structural Design of Tall Buildings, 10(5), 311-320.

[33] Agrawal, A. K., & Amjadian, M. (2016). Seismic component devices. In Innovative bridge design handbook (pp. 531-553). Butterworth-Heinemann.

[34] Filiatrault, A., & Christopoulos, C. (2006). Principles of passive supplemental damping and seismic isolation.

[35] Impollonia, N., & Palmeri, A. (2018). Seismic performance of buildings retrofitted with nonlinear viscous dampers and adjacent reaction towers. Earthquake Engineering & Structural Dynamics, 47(5), 1329-1351.

[36] McKenna, F. (2011). OpenSees: a framework for earthquake engineering simulation. *Computing in Science & Engineering*, 13(4), 58-66.

[37] Scozzese, F., Tubaldi, E., & Dall'Asta, A. (2020). Assessment of the effectiveness of Multiple-Stripe Analysis by using a stochastic earthquake input model. *Bulletin of Earthquake Engineering*, 1-37.

[38] Seleemah, A.A. and Constantinou, M.C. (1997). *Investigation of seismic response of buildings with linear and nonlinear fluid viscous dampers.* Report No. NCEER-97-0004.

New York: National Center for Earthquake Engineering Research, State University of New York at Buffalo.

[39] Hanson, R.D. and Song, T.T. (2001). *Seismic design with supplemental energy dissipation devices*. Oakland, California: Earthquake Engineering Research Institute.

[40] Fajfar, P. (2018). Analysis in seismic provisions for buildings: past, present and future. *Bulletin of Earthquake Engineering*, **16**, 2567-2608. DOI:°10.1007/s10518-017-0290-8

[41] Gkimprixis, A., Tubaldi, E., & Douglas, J. (2019). Comparison of methods to develop risk-targeted seismic design maps. *Bulletin of earthquake engineering,* 17(7), 3727-3752.